J Braz. Soc. Mech. Sci. Eng. (2015) 37:641–655
DOI 10.1007/s40430-014-0193-4

TECHNICAL PAPER

Influence of surfactant and graphite powder concentration on electrical discharge machining of PH17-4 stainless steel

V. Vikram Reddy · A. Kumar · P. Madar Valli · Ch Sridhar Reddy

Received: 15 November 2013 / Accepted: 6 May 2014 / Published online: 31 May 2014

Abstract In the present work, an investigation has been made into the electrical discharge machining process (EDM) when both graphite powder and surfactant-mixed dielectric fluid were used during EDM of precipitation hardening stainless steel PH17-4. The addition of graphite powder in the dielectric fluid results in uniform distribution of discharge, which improves surface finish. However, agglomeration of graphite particles is found in the dielectric due to the electrostatic forces among the graphite powder particles. The addition of surfactant in the dielectric increases dielectric conductivity and in turn reduces relay time of discharge. This increases actual discharge time, which results in more material removal. At the same time, uniform distribution of graphite powder particles in the dielectric fluid is achieved. This leads to increase in discharge frequency, which results in increase in material removal rate and surface finish. Taguchi parameter design approach was used to get an optimal parametric setting of EDM process parameters namely: peak current, surfactant concentration and graphite powder concentration that yields to optimal process performance characteristics such as material removal rate, surface roughness, white layer thickness and surface crack density. Individual effect of process parameters on performance characteristics was also studied. To identify the significance of parameters on measured response, the analysis of variance has been carried out. Further, mathematical models were developed by performing nonlinear regression analysis to predict process performance characteristics. Confirmation tests were conducted at their respective optimal parametric settings to verify the predicted optimal values of performance characteristics.

Keywords EDM · Surfactant · Graphite powder · Material removal rate · Surface roughness · White layer thickness · Surface crack density

Technical Editor: Alexandre Mendes Abrao.

V. V. Reddy (✉)
Mechanical Engineering Department, Jayamukhi Institute of Technological Sciences, Warangal 506331, AP, India
e-mail: vaddi.vikramreddy@gmail.com

A. Kumar
Mechanical Engineering Department, N.I.T, Warangal, AP, India

P. M. Valli
Industrial Engineering Department, GITAM Institute of Technology, Visakhapatnam, AP, India

C. S. Reddy
Mechanical Engineering Department, JNTU, Karimnagar, AP, India

1 Introduction

Electrical discharge machining (EDM) is widely used in manufacturing industry to make dies of complex cavities. In EDM, the material is removed primarily through the conversion of electrical energy into thermal energy through a series of discrete electrical discharges occurring between tool and work piece when both are immersed inside a dielectric medium and are separated by a small gap. The material is removed from the work piece by localized melting and even vaporization of material by high temperature spark. This causes many defects such as micro cracks, porosity, residual stress and the white layer, which are found on the machined surface. The reason for the defects is due to rapid high temperature melting and subsequent rapid cooling during machining process. Further,

there is no physical contact between the tool and work piece, which eliminates mechanical stresses, chatter and vibration problem during machining that enables EDM to machine brittle material [1]. In general, material removal rate (MRR) improves with decreased surface finish. On the other hand, improved surface finish is obtained with decreased MRR during EDM. It is difficult to achieve both improved MRR and decreased surface roughness (SR) in EDM simultaneously. Many researchers attempted various techniques such as rotary EDM, vibratory-assisted EDM and powder mixed EDM (PMEDM) to solve the above problems.

Precipitation hardening stainless steel PH17-4/AISI 630/UNSS17400 having high strength and high corrosive resistant material of reasonable cost would retain considerable strength up to moderately elevated temperature, and this steel is hardened by precipitation by heat treatment. This steel is extensively used in marine, aero space, chemical, petro chemical, food processing, paper and general metal work industries. Further PH17-4 steel has several applications such as: pump shafts, aircraft fittings, valve stems, hydraulic fittings, studs, bushings, screws, fasteners and couplings, wear rings, rollers, food handling equipment. However, PH17-4 stainless steel is difficult to machine with conventional machining processes owing to its high hardness value. Hence it is important to investigate the characteristics of electric discharge machining of PH17-4 stainless steel.

The rotary motion of work piece improves the dielectric circulation through the discharge gap results increasing in MRR [3]. Machining characteristics of EN8 steel with disc type rotating copper electrode during rotary EDM have been studied [4]. The effect of axial vibration of tool along with rotation on MRR and tool wear rate (TWR) during EDM was studied [5]. The improvement in performance of EDM was noticed with mixing of silicon powder in dielectric [6]. The optimization of process parameters such as current, pulse on time, concentration of Silicon powder, duty cycle of PMEDM has done with considering responses as MRR and SR using response surface methodology (RSM) [2]. The semiempirical model was proposed to estimate residual stresses developed during EDM and reported the pattern of residual stress distribution [7]. The significant increase in the performance of PMEDM over conventional EDM was noticed with the addition of silicon powder into dielectric fluid [8]. The comparison between the electrode wear along the cross section of an electrode with electrode wear along its length during EDM was studied [9]. The effect of parameters on SR, MRR during EDM of EN31 tool steel using copper, brass and graphite as electrodes was studied, and different patterns of the heat affected zone (HAZ) are also observed for all the specimens machined by three different electrodes [10]. The effect of peak current, pulse on time and gap voltage on the responses that are MRR and SR with different tool electrodes namely copper, brass and graphite was studied [11]. The influences of EDM input parameters namely pulse on time and pulse current on MRR, EWR and SR, white layer thickness (WLT) and depth of heat affected zone (DHAZ) were studied [12]. PMEDM of γ-TiAl by means of adding different powders such as aluminum, chrome, silicon carbide, graphite and iron to the dielectric to find its effect on SR, topography, MRR, electro chemical corrosion resistance of machined samples was studied [13]. The improvement in surface properties (improved surface roughness, increased micro hardness) with Si, W and graphite powders mixed in dielectric in PMEDM process was noticed [14].

From the literature, it has been observed that no extensive work has been carried out in the field of EDM of precipitation hardening stainless steel PH17-4 using both graphite powder and surfactant-mixed dielectric fluid. So far, no work was carried out to know the effect of adding surfactant and graphite powder to the dielectric during EDM of PH17-4 as a work material (Fig. 1).

The mechanism of material removal is shown in Fig. 2. The addition of surfactant in the dielectric results in the absorption of hydrophilic head group on the surface of graphite powder, debris and carbon dregs, and hydrophobic tail would extend to the dielectric fluid. Thus, surfactant molecules act as steric barrier to separate the agglomerated graphite powder, debris and carbon dregs due to electrostatic forces and disperse them uniformly within the dielectric. It minimizes the bridge effect and provides better distribution of discharge energy resulting in increase in discharge frequency. On the other hand, the addition of surfactant in the dielectric increases dielectric conductivity which reduces bridging time. This causes reduction in relay time of discharge that finally increases actual discharge time in the entire discharge process. This causes increase in discharge energy, which in turn results in overall increase in MRR and improvement in surface finish.

Based on the literature survey and our preliminary investigations, the parameters chosen as input parameters are peak current I (A), surfactant concentration SC (g/lt.) and graphite powder concentration PC (g/lt). The aim of the present work is to identify the significant effect of the above chosen input parameters on EDM characteristics such as material removal rate (MRR), surface roughness (SR), White layer thickness (WLT) and surface crack density (SCD) and also to find the optimal parametric settings to maximize MRR and to minimize the SR, WLT and SCD of PH 17-4 stainless steel. Further mathematical models were developed using nonlinear regression analysis to predict chosen machining characteristics in terms of chosen input parameters.

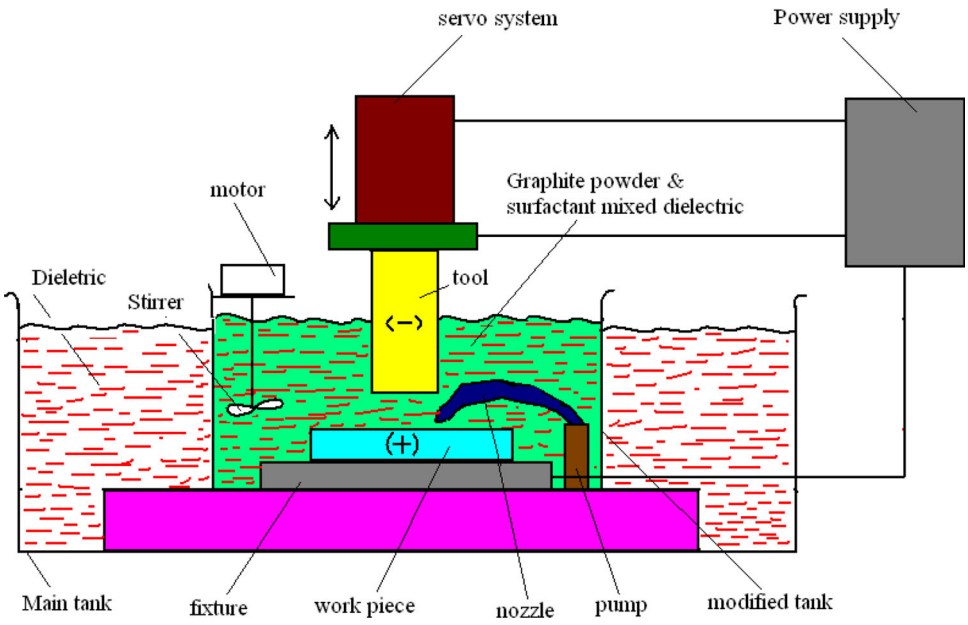

Fig. 1 Schematic diagram of experimental set up

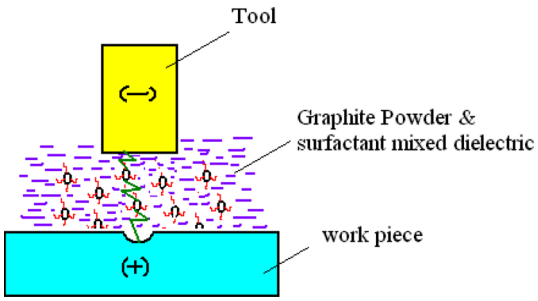

Fig. 2 Mechanism of material removal

2 Experimental setup, procedure and equipment

For conducting experiments, the work material PH17-4 stainless steel ingot is cut into the sample pieces with the dimensions of 80 × 30 × 6 mm by means of wire-cut EDM process by setting very low peak current and pulse on time values. The hardness of the material is measured at different points, and average hardness value is found to be 41.7 HRC. The chemical composition of the PH17-4 stainless steel is shown in Table 1. The mechanical and physical properties of PH17-4 steel are presented in Table 2. The electrolyte copper of diameter ø14 mm and length 70 mm is selected as tool material, and its physical properties are presented in the Table 3. The dielectric fluid used to conduct all the experiments is commercial EDM oil grade SAE450 and its viscosity at 38 °C is 2.16 cts and dielectric strength is 45 kv/mm. Considering safety and pollution issues, the surfactant with least irritation non-ionic SPAN20 is chosen to add into the dielectric for all the experiments. This is chosen for the reason that the conductivity of dielectric fluid increases with its concentration and also due to high value of HLB [16]. Chemical properties of SPAN20 are presented in the Table 4. Owing to higher thermal conductivity, low electrical resistivity and high melting point, the graphite powder (particle size 20–30 μm) is chosen to add into the dielectric fluid with surfactant. All the experiments are conducted on die-sinking EDM machine of FORMATICS 50 model, which is equipped with ELECTRONICA PRS 20 controller. Modified working fluid circulating system has been designed for experimentation. In modified system, a separate tank mounted with micro pump is installed for better circulation of graphite powder and surfactant-mixed dielectric fluid. A motorized stirring system is incorporated to avoid settling of powder particles. Schematic diagram of modified experimental setup is shown in Fig. 1. The design of experiment (DOE) chosen for this study was a Taguchi L9 orthogonal array, by conducting a total number of 9 experimental runs. Each experimental run was repeated three times. Machining time for conducting each experiment is 3 min. The work pieces and electrodes were cleaned and polished before machining. The work piece was firmly clamped in the vice and immersed in the dielectric. The chosen input factors and corresponding levels for this study are presented in the Table 5. The chosen experimental conditions are presented in the Table 6.

The Taguchi method uses S/N (Signal to Noise) ratio to measure the deviation of performance characteristics from the desired values. There are three categories of S/N ratios depending on the types of characteristics like higher is the

Table 1 Chemical composition of PH17-4 stainless steel

Element	C	Mn	Si	P	S	Cr	Ni	Cu	Nb	Fe
Wt %	0.029	0.783	0.344	0.038	0.022	15.305	3.76	3.014	0.205	Balance

Table 2 Properties of PH17-4 stainless steel

Density	7.8 (g/cm^3)
Specific capacity	400 (J/kg °k)
Thermal conductivity	18.4 (W/m °k)
Electrical resistivity	0.08×10^{-6} Ω m
Modulus of elasticity	196 G Pa

Table 3 Physical properties of electrolyte copper

Density	8.95 (g/cm^3)
Specific capacity	383 (J/kg °C)
Thermal conductivity	394 (W/m °C)
Electrical resistivity	1.673×10^{-8} Ω m
Melting point	1,083 °C

Table 4 Surfactant SPAN20 chemical properties

Formula	$C_{18}H_{34}O_6$
Molecular weight	346.47 g/mol
HLB value	8.6
Water content (%)	<1.5
Acidic value	4–8
Saponification value	158–170
Heavy metal (PPM)	≤10
Iodine value	4–8

Table 5 Input process parameters and their levels

Parameter	Level 1	Level 2	Level 3
Peak current *I* (A)	10	15	20
Surfactant concentration SC (g/lt)	4	6	8
Powder concentration PC (g/lt)	4.5	9	13.5

best (HB), lower is the best (LB) and nominal is the best (NB). MINITAB 16 software was used to analyze the experimental data. A digital weighing balance (citizen) having capacity up to 300 g with a resolution of 0.1 mg is used for weighing the work pieces before machining and after machining. Then the material removal rate (MRR) is calculated as follows.

$$\mathrm{MRR}\,(\mathrm{mm}^3/\mathrm{min}) = \Delta W/\rho w \times t \quad (1)$$

where ΔW is the weight difference of work piece before and after machining (g), ρw is density of work material (g/mm^3) and t is machining time in minutes. SR of the machined

Table 6 Experimental conditions

Working conditions	Description
Work piece	PH17-4 stainless steel (80 mm × 30 mm × 6 mm)
Electrode	Electrolyte copper Ø 14 mm and length 70 mm
Dielectric	Commercial EDM Oil grade SAE 450 + Gr powder + surfactant SPAN20
Flushing	Side flushing with pressure 0.5 MPa
Gr. Powder particle size	20–30 μm
polarity	Normal
Supply voltage	110 V
Gap voltage	70 V
Pulse duration	65 μs
Pulse off time	48 μs
Machining time	3 min

work pieces is measured using Talysurf surface roughness tester. The SR is represented by the center line average method (Ra). Roughness measurements are carried out in the transverse direction on machined surface with sampling length of 0.8 mm and are repeated three times, and average values are calculated. In order to determine the WLT after conducting experiments, the machined specimens are sectioned transversely by wire-cut EDM and polished subsequently with silicon carbide papers of grit sizes 120, 220, 320, 400 and 800 and then polished on double disk grinder by applying diamond paste. In order to expose the white layer structure and boundary line, etchant solution (1 g picric acid, 75 ml methyl alcohol, 15 ml hydrochloric acid) was applied on the polished surface of specimen for a period of 1 min. Then the surface is cleaned with water and dried further. The micrograph of white layer was then seen under scanning electron microscope (SEM) (Model Hitachi S3700 N model) for the analysis. Further WLT has been obtained by taking the average values measured at five different points. Further, the calculation of SCD was carried out by measuring the total length of cracks in the white layer area and dividing this total length of cracks by the area of the WLT in SEM micrograph.

3 Results and discussion

It is possible to sort out each process parameter on response at different levels since the experiments are designed in

Table 7 Experimental results for the EDM performance characteristics MRR, SR, WLT and SCD

exp	Input parameters			Performance characteristics and their corresponding S/N ratios							
	I (A)	SC (g/lt)	PC (g/lt)	MRR (mm^3/min)[a]	S/N MRR	SR (μm)[a]	S/N SR	WLT (μm)[a]	S/N WLT	SCD (μm/$μm^2$)[a]	S/N SCD
1	10	4	4.5	29.04	29.26	3.1	−9.82	14.65	−23.31	0.01	40
2	10	6	9	37.48	31.47	3.7	−11.36	16.44	−24.32	0.023	32.76
3	10	8	13.5	31.11	29.85	3.6	−11.12	17.24	−24.73	0.029	30.75
4	15	4	9	42.97	32.66	6.8	−16.65	16.88	−24.54	0.021	33.55
5	15	6	13.5	53.17	34.51	7.6	−17.61	19.35	−25.73	0.043	27.33
6	15	8	4.5	43.60	32.79	6.4	−16.12	21.43	−26.62	0.024	32.39
7	20	4	13.5	52.09	34.33	6.64	−16.44	22.95	−27.21	0.032	29.89
8	20	6	4.5	60.76	35.67	7.8	−17.84	27.12	−28.66	0.037	28.63
9	20	8	9	54.01	34.64	7.5	−17.50	24.70	−27.85	0.028	31.05

[a] Average of three values

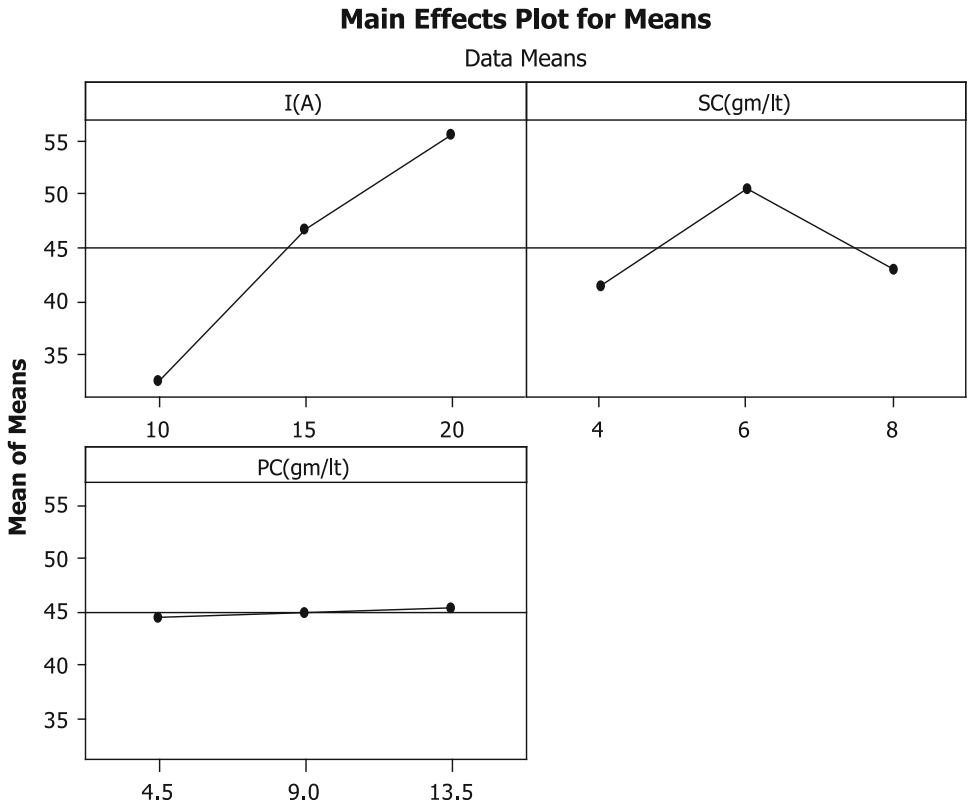

Fig. 3 The effect of process parameters on means of MRR

orthogonal nature. The raw data of various responses collected after conducting experiments for each trial were transferred into their respective S/N ratio values.

3.1 Effect of parameters on material removal rate (MRR)

The average values of MRR, SR, WLT and SCD for each trial (run) and their respective S/N ratio values are presented in the Table 7. From the Figs. 3, 4, it is observed that the parameters such as peak current, surfactant concentration and graphite powder concentration considerably affect both the mean and variation in MRR values (S/N ratio). From the response graphs (Figs. 3, 4), it has been observed that MRR increases significantly with increase in peak current values from 10 to 20 A. The peak current directly influences the discharge energy available in the inter-electrode gap. The increase in peak current causes increase in spark energy, which further results into higher current density. This increased current density rapidly overheats the work piece

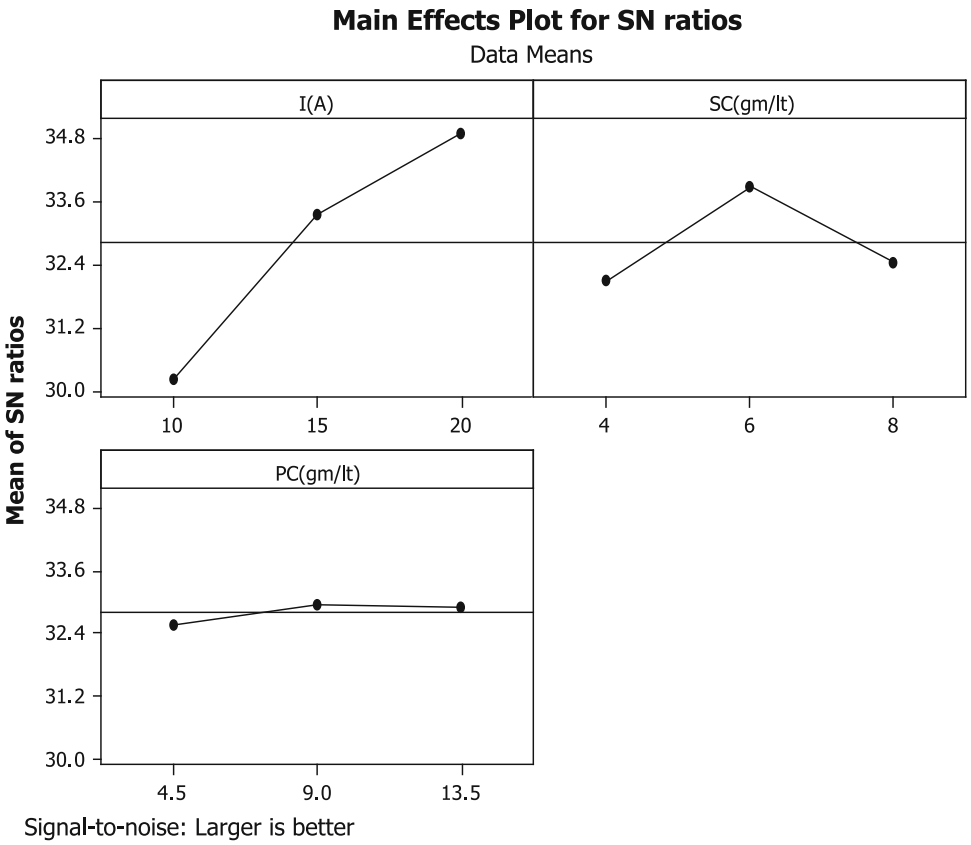

Fig. 4 The effect of process parameters on S/N Ratio of MRR

and thus increases the MRR at higher peak current conditions [4]. Further, as current increases, discharge strikes the surface of work piece intensively, which creates an impact force on the molten material in the molten puddle, and this results in the ejection of more material out of the crater [12]. Another observation from the present experiment is that when surfactant concentration is increased up to 6 g/lt, the MRR increases. It starts getting decreased when surfactant concentration is further increased up to 8 g/lt. The addition of surfactant (SPAN20) increases conductivity of EDM oil, which results in shorter bridging time that causes shorter relay time of discharge. This leads to an increase in the actual discharge time, resulting in increase in MRR. On the other hand, the addition of surfactant in the EDM oil retards the agglomeration of debris, carbon dregs and graphite powder particles due to electrostatic forces during machining. Uniform distribution of graphite powder particles achieved in the inter-electrode gap minimizes the bridge effect that causes better distribution of discharge energy resulting in overall increase in MRR [15]. The increase in surfactant concentration from 6 to 8 g/lt decreases the metal removal rate. This may be due to increase in conductivity of the dielectric fluid in the gap with an addition of surfactant to it. This results in dissipation of more amount of energy into the dielectric fluid. This causes reduction in energy available at work piece, which reduces MRR [13].

Table 8 Analysis of variance (ANOVA) for raw data MRR

Source	DF	Seq SS	Adj SS	Adj MS	*F*	*P*
I (A)	2	811.24	811.24	405.62	525.89	0.002
SC (g/lt)	2	142.42	142.42	71.21	92.32	0.011
PC (g/lt)	2	1.51	1.51	0.75	0.98	0.506
Error	2	1.54	1.54	0.77		
Total	8	956.71				

$S = 0.878237$, $R^2 = 99.84$ %, R^2 (adj) $= 99.36$ %

Further, it is also noticed that increase in graphite powder concentration increases the MRR. This may be due to the fact that the addition of conductive powder particles to the dielectric fluid lowers the breakdown strength of the dielectric. The accumulated powder particles in the gap form a bridge in the discharge gap due to electrostatic forces between the electrodes. These particles will be well distributed in the gap due to addition of surfactant in the dielectric fluid. This results in uniform dispersion of energy into several increments. It means there is an increase in sparking frequency, which in turn increases in the overall metal removal rate. The Fig. 4 suggests that when peak current is at 20 A (level 3), surfactant concentration at 6 g/lt (level 2) and powder concentration at 9 g/lt (level 2) provide maximum MRR.

Table 9 Estimated Regression Coefficients for MRR

Term	Coef	SE Coef	T	P
Constant	−82.7896	7.79496	−10.621	0.009
I (A)	5.3060	0.74865	7.087	0.019
SC (g/lt)	25.3828	1.87163	13.562	0.005
PC (g/lt)	−0.0144	0.55773	−0.026	0.982
I^2	−0.0999	0.02484	−4.024	0.057
SC^2	−2.0832	0.15525	−13.418	0.006
PC^2	0.0069	0.03067	0.225	0.843

$S = 0.878237$, PRESS = 31.2377, $R^2 = 99.84$ %, R^2 (pred) = 96.73 %, R^2 (adj) = 99.36 %

Table 10 Predicted values of MRR using regression model

EXP	I (A)	SC (g/lt)	PC (g/lt)	MRR (mm^3/min)	FIT MRR	RESI
1	10	4	4.5	29.04	28.55	0.49
2	10	6	9	37.48	38.01	−0.52
3	10	8	13.5	31.11	31.08	0.03
4	15	4	9	42.97	42.94	0.03
5	15	6	13.5	53.17	52.67	0.49
6	15	8	4.5	43.60	44.12	−0.52
7	20	4	13.5	52.09	52.61	−0.52
8	20	6	4.5	60.76	60.73	0.03
9	20	8	9	54.01	53.52	0.49

Analysis of variance (ANOVA) of the data presented in the Table 8 reveals the significance of input parameters on MRR, which is as follows. The most significant, significant and less significant parameters are peak current, surfactant concentration and powder concentration, respectively. Optimum value of MRR is calculated as 61.08 mm^3/min, and corresponding S/N ratio is 36.09 at its optimal parameter settings. Further mathematical model has been developed using nonlinear regression analysis to predict the MRR values. The regression equation is

$$\mathrm{MRR} = -82.7896 + 5.3060I + 25.3828\mathrm{SC} - 0.0144\mathrm{PC} - 0.0999I^2 - 2.0832\mathrm{SC}^2 + 0.0069\mathrm{PC}^2 \quad (2)$$

The regression coefficients of the model are presented in the Table 9. The predicted values of MRR using regression Eq. (2), and corresponding residuals are presented in the Table 10. The values of R^2 (99.8 %) and R^2 adj (99.3 %) of the model are in the acceptable range of variability in predicting MRR values.

3.2 Effect of parameters on surface roughness (SR)

The average values of SR for each trial and their respective S/N ratio values are presented in the Table 7. The individual effect of process parameters such as peak current, surfactant concentration and graphite powder concentration on the mean values of SR, and S/N ratio for SR are presented in Figs. 5 and 6. Further it is observed from the Figs. 5 and 6 that there is an increase in SR value with increase in peak current. The reason is that the increase in peak current causes increases in spark energy consequently deeper, and larger craters are formed, which increase the SR. It is also noticed that initially SR increases with the increase in powder concentration. It starts decreasing with further increase in powder concentration. In powder mixed electrical discharge machining, the addition of electrically conductive powders into dielectric fluid causes decrease in its insulating strength, leading to widening of the gap between electrodes to stabilize the discharge condition. The enlarged and widened discharged channel reduces the electrical density on the machining spot and thus generates shallow craters and lower SR. On the other hand, with increase in thermal conductivity of dielectric due to the addition of powders, more heat is dissipated into dielectric. Subsequently, the level of heat energy available at work surface is decreased [13]. The small increase in SR value is observed with the increase in powder concentration from 4.5 to 9 g/lt. A very small decrease in SR value is noticed when there is further increase in powder concentration from 9 to 13.5 g/lt. Whereas, increase in surfactant concentration from 4 to 6 g/lt increases the SR value from 5.513 to 6.367 μm, and further increase in surfactant concentration to 8 g/lt results in decrease in SR value to 5.833 μm. The reason for the above is that there is an increase in dielectric conductivity with increase in surfactant concentration. This causes more concentrated spark energy, which results in increased SR. On the other hand, increase in surfactant concentration causes increase in conductivity of dielectric, and at the same time, the presence of well-distributed powder particles, debris and carbon dregs results in uniform distribution of spark energy, which creates reduced SR. From Fig. 5, it is noticed that input parameters namely: peak current, surfactant concentration and graphite powder concentration appreciably affect the mean values of SR.

Figure 6 suggests that minimum SR value is attained when peak current is at 10 A (level 1), surfactant concentration at 4 g/lt (level 1) and graphite powder concentration at 4.5 g/lt (Level 1). Further, optimum SR value is calculated as 2.93 μm, and corresponding S/N ratio is −9.78. It is observed from the Table 11 that the peak current has most significant effect on SR, whereas other two parameters, surfactant concentration and powder concentration, do not have that much affect on SR. Further, the mathematical model has been developed using nonlinear regression analysis to predict the SR values.The regression equation is

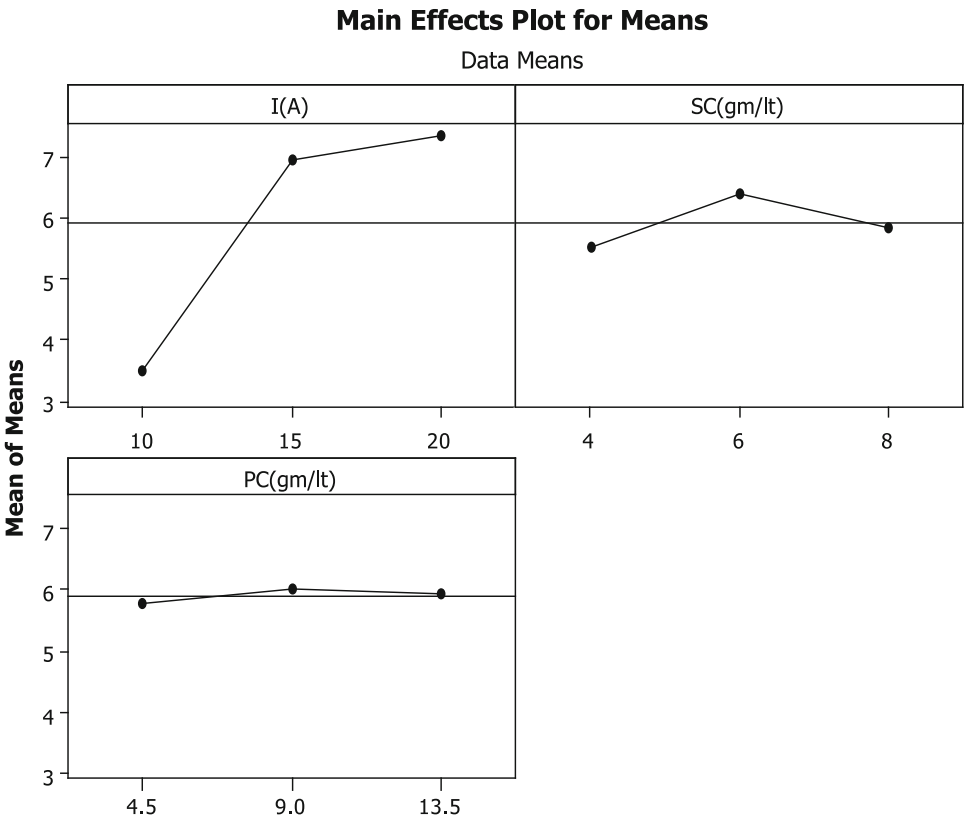

Fig. 5 The effect of process parameters on means of SR

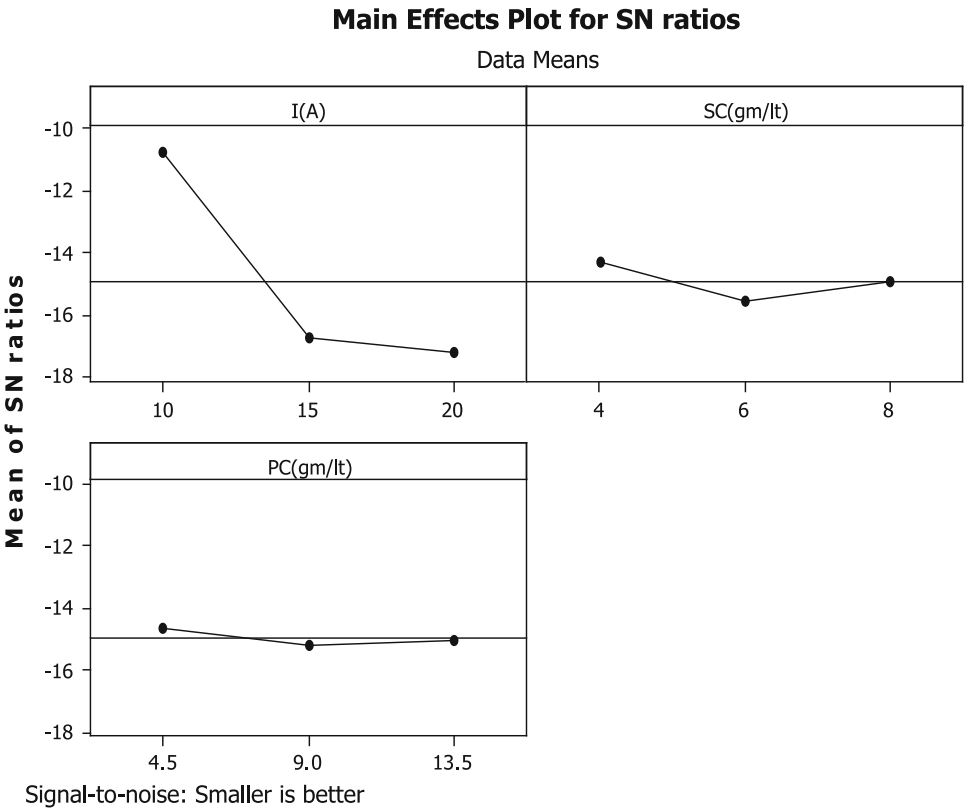

Fig. 6 The effect of process parameters on S/N Ratio of SR

Table 11 Analysis of variance (ANOVA) for raw data SR

Source	DF	Seq SS	Adj SS	Adj MS	*F*	*P*
I (A)	2	26.9590	26.9590	13.4795	56.91	0.017
SC (g/lt)	2	1.1150	1.1150	0.5575	2.35	0.298
PC (g/lt)	2	0.0897	0.0897	0.0448	0.19	0.841
Error	2	0.4737	0.4737	0.2368		
Total	8	28.6374				

$S = 0.486667$, $R^2 = 98.35$ %, R^2 (adj) = 93.38 %

Table 12 Estimated regression coefficients for SR

Term	Coef	SE Coef	*T*	*P*
Constant	−19.6422	4.31950	−4.547	0.045
I (A)	2.2367	0.41486	5.391	0.033
SC (g/lt)	2.1600	1.03714	2.083	0.173
PC (g/lt)	0.1474	0.30906	0.477	0.680
I^2	−0.0617	0.01377	−4.485	0.046
SC^2	−0.1733	0.08603	−2.015	0.182
PC^2	−0.0071	0.01699	−0.417	0.717

$S = 0.486667$, PRESS = 9.5922, $R^2 = 99.35$ %, R^2 (pred) = 66.50 %, R^2 (adj) = 93.38 %

Table 13 Predicted values of SR using regression model

EXP	*I* (A)	SC (g/lt)	PC (g/lt)	SR (μm)	FIT SR	RESI
1	10	4	4.5	3.1	2.93	0.16
2	10	6	9	3.7	4.02	−0.32
3	10	8	13.5	3.6	3.43	0.16
4	15	4	9	6.8	6.63	0.16
5	15	6	13.5	7.6	7.43	0.16
6	15	8	4.5	6.4	6.72	−0.32
7	20	4	13.5	6.64	6.96	−0.32
8	20	6	4.5	7.8	7.63	0.16
9	20	8	9	7.5	7.33	0.16

$$\mathrm{SR} = -19.6422 + 2.2367I + 2.16\mathrm{SC} + 0.1474\mathrm{PC} - 0.0617I^2 - 0.1733\mathrm{SC}^2 - 0.0071\mathrm{PC}^2 \quad (3)$$

The regression coefficients are presented in the Table 12. The predicted values of SR using regression Eq. (3), and corresponding residuals are presented in the Table 13. The values of R^2 (98.35 %) and R^2 adj (93.38 %) of the model are in the acceptable range of variability in predicting SR values.

3.3 Effect of process parameters on white layer thickness (WLT)

The features of electrical discharge machining (EDM) such as large spark energy range, variation in surface finish, extreme cooling rates, chemical surface impurities from electrode and dielectric (carbon is more important contaminant) and a recast layer attract more attention for surface integrity of electrical discharge machined surfaces. The HAZ produced by the EDM contains an upper layer known as white layer or recast layer followed by phase transformation zone and conversion zone. WLT was measured for all machined samples by taking SEM photographs on sectioned machined surfaces on the edge of machined surface. The average values of WLT measured from SEM photographs, and their corresponding S/N ratio values are presented in the Table 7. Further, SEM photographs of samples of all experimental runs are presented in Fig. 9. From the Figs. 7 and 8, it is observed that the parameters such as peak current, surfactant concentration and graphite powder concentration considerably affect both the mean and variation in WLT values (S/N ratio). From the response graphs (Figs. 7, 8), it has been observed that WLT increases significantly with increase in peak current. This can be attributed to the fact that increases in peak current causes increase in discharge density and decrease in flushing efficiency. Concentrated high discharge energy increases the amount of formation of molten metal. Consequently, decrease in flushing condition causes formation of more re-solidified material resulting in increase in WLTs. It is also observed from Fig. 7 that the WLT increases insignificantly with increase of surfactant concentration in dielectric fluid. The addition of surfactant to the dielectric improves its conductivity and at the same time lowers its viscosity resulting in more easy flow of dielectric into the inter-electrode gap. As a result, the increase in dreg removal rate leads to improved flushing conditions. At the same time, the addition of powder particles into the dielectric results in uniform distribution of discharge energy, which lowers the amount of penetrated heat energy into the work surface. This leads to decrease in thickness of white layer. However, with increase in surfactant concentration, there will be a slight increase in WLTs. This may be due to the reason that the decrease in relay time of discharge results in increase in actual discharge time that leads to more heat penetration into the work causing increase in WLT.

It is also observed from Fig. 7 that value of WLT is decreased with increase in powder concentration from 4.5 to 9 g/lt and then increased slightly with further increase in powder concentration from 9 to 13.5 g/lt. The adding of graphite powder into the dielectric fluid lowers the discharge energy for single spark and increases sparking frequency, which reduces the amount of heat available at work surface. This results in reduced WLT. On the other hand, due to increased conductivity of dielectric in the gap, more amount of heat is dissipated to dielectric. This results in formation of less amount of molten metal, which lowers

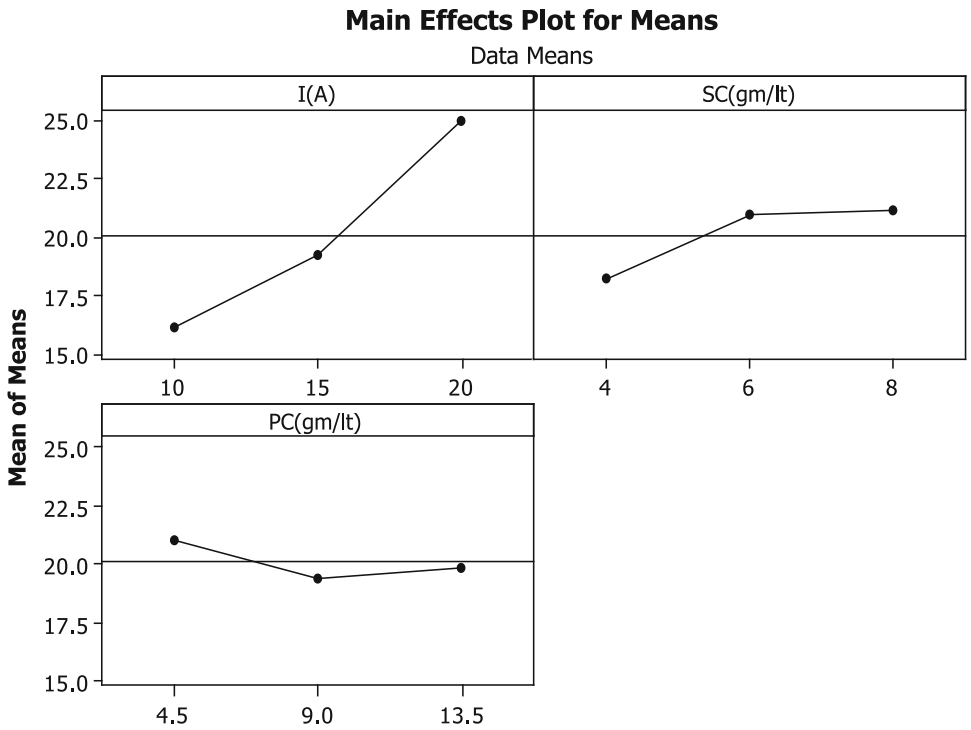

Fig. 7 The effect of process parameters on means of WLT

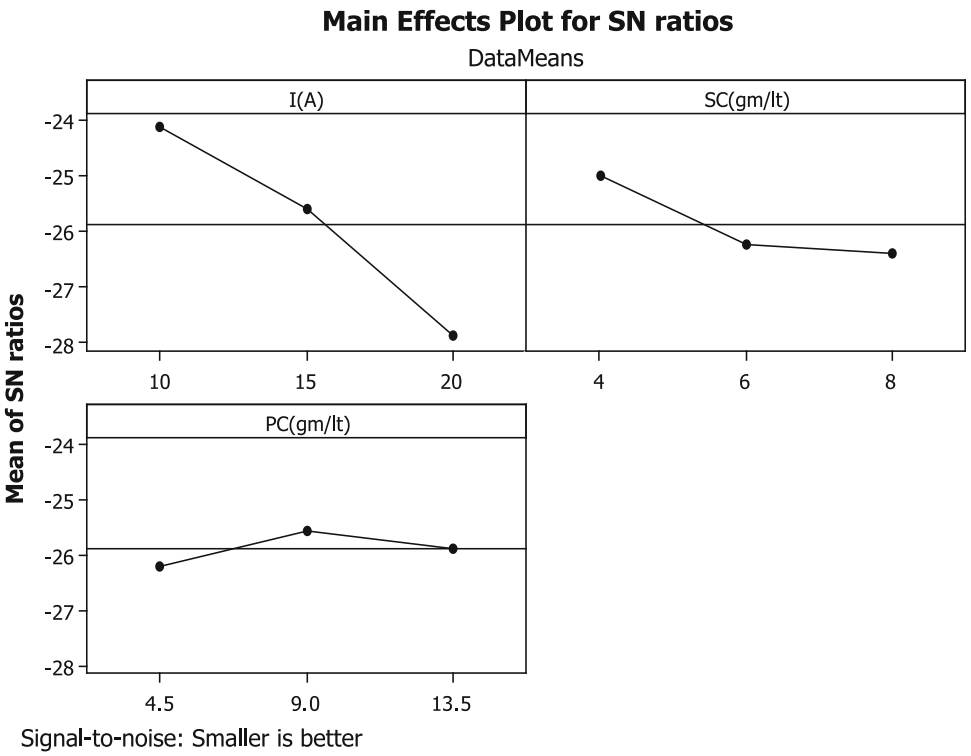

Fig. 8 The effect of process parameters on S/N Ratio of WLT

the WLTs. Further, insignificant increase in the WLTs is observed with increase in powder concentration in the dielectric from 9 to 13.5 g/lt. This may be due to the presence of more concentration of powder particles in the gap. This results in unstable discharge that may cause increase in WLTs.

It is noticed from the Fig. 8 that minimum WLT value is obtained when peak current is at 10 A (level 1), surfactant

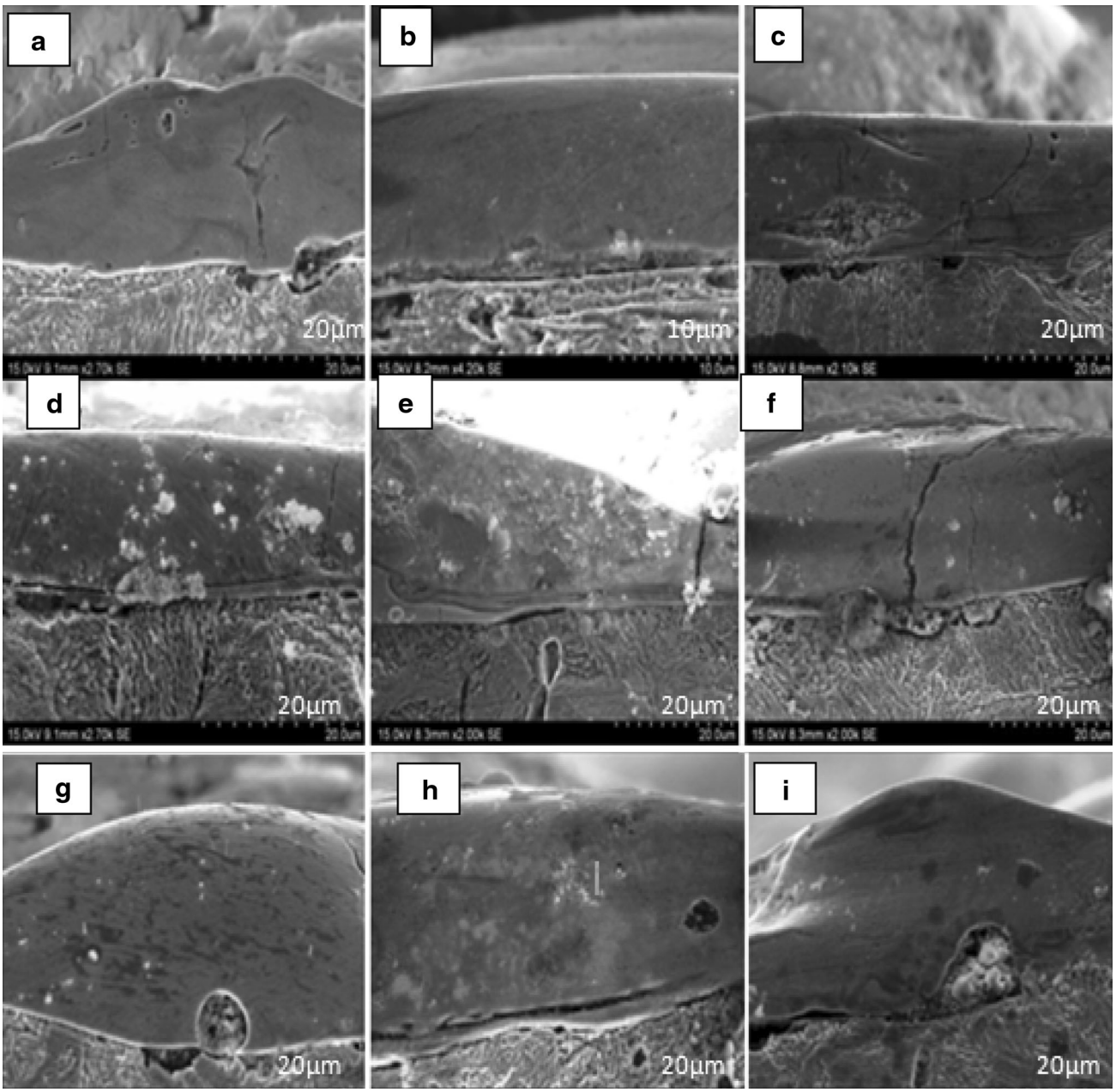

Fig. 9 SEM Photographs of Sectioned samples at **a** $I = 10$A, SC = 4 g/lt, PC = 4.5 g/lt, WLT = 14.6549 µm **b** $I = 10$A, SC = 6 g/lt, PC = 9 g/lt, WLT = 16.4469 µm, **c**: $I = 10$A, SC = 8 g/lt, PC = 13.5 g/lt, WLT = 17.2464 µm, **d** $I = 15$A, SC = 4 g/lt, PC = 9 g/lt, WLT = 16.8834 µm, **e** $I = 15$A, SC = 6 g/lt, PC = 13.5 g/lt, WLT = 19.3585 µm, **f** $I = 15$A, SC = 8 g/lt, PC = 4.5 g/lt, WLT = 21.4351 µm, **g** $I = 20$A, SC = 4 g/lt, PC = 13.5 g/lt, WLT = 22.9543 µm, **h** $I = 20$A, SC = 6 g/lt, PC = 4.5 g/lt WLT = 27.1256 µm, **I** $I = 20$A, SC = 8 g/lt, PC = 9 g/lt, WLT = 24.7091 µm

concentration at 4 g/lt (level 1) and graphite powder concentration at 9 g/lt (Level 2). Further optimum WLTs value is calculated as 13.44 µm, and corresponding S/N ratio as −22.94 at above optimal parameter setting. It is also observed from the Table 14 that peak current is the most significant parameter followed by surfactant concentration and powder concentration, which are significant parameter and less significant parameter, respectively, affecting of WLT.

Further, nonliner regression analysis is performed from the experimental data to develop mathematical model to predict response variable WLT. The regression coefficients of the model are presented in the Table 15. Further, mathematical equation to predict WLT is

Table 14 Analysis of variance (ANOVA) for raw data WLT

Source	DF	Seq SS	Adj SS	Adj MS	*F*	*P*
I (A)	2	119.885	119.885	59.942	97.56	0.010
SC (g/lt)	2	16.732	16.732	8.366	13.62	0.068
PC (g/lt)	2	4.719	4.719	2.360	3.84	0.207
Error	2	1.229	1.229	0.614		
Total	8	142.565				

$S = 0.783845$, $R^2 = 99.14$ %, R^2 (adj) = 96.55 %

Table 15 Estimated Regression Coefficients for WLT

Term	Coef	SE Coef	*T*	*P*
Constant	7.08826	6.95716	1.019	0.415
I (A)	−0.67528	0.66819	−1.011	0.419
SC (g/lt)	4.73089	1.67047	2.832	0.105
PC (g/lt)	−1.12742	0.49778	−2.265	0.152
I^2	0.05189	0.02217	2.340	0.144
SC^2	−0.33245	0.13857	−2.399	0.139
PC^2	0.05511	0.02737	2.013	0.182

$S = 0.783845$, PRESS = 24.8838

$R^2 = 99.14$, R^2 (pred) = 82.55 %, R^2 (adj) = 96.55 %

Table 16 Predicted values of WLT using regression model

EXP	*I* (A)	SC (g/lt)	PC (g/lt)	WLT (μm)	FIT WLT	RESI
1	10	4	4.5	14.65	15.17	−0.51
2	10	6	9	16.44	16.25	0.18
3	10	8	13.5	17.24	16.91	0.32
4	15	4	9	16.88	16.55	0.32
5	15	6	13.5	19.35	19.87	−0.51
6	15	8	4.5	21.43	21.24	0.18
7	20	4	13.5	22.95	22.76	0.18
8	20	6	4.5	27.12	26.79	0.32
9	20	8	9	24.70	25.22	−0.51

$$\begin{aligned} \text{WLT} =& 7.08826 - 0.67528I + 4.73089\text{SC} \\ & - 1.12742\text{PC} + 0.05189I^2 - 0.33245\text{SC}^2 \\ & + 0.05511\text{PC}^2 \end{aligned} \quad (4)$$

The predicted values of WLT using mathematical Eq. (4), and corresponding residuals are presented in the Table 16. The R^2 (99.14 %) and R^2 adj (96.55 %) values of the model are in acceptable level.

3.4 Effect of process parameters on surface crack density (SCD)

Generation of thermal stress having magnitude of more than fracture strength of work material in an EDM process results in crack formation. Cracking is one of the most significant surface defects, which lead to a reduction in the material resistance, fatigue and corrosion under tensile loading conditions. Since it is not easy to quantify in terms of width, length or depth or even by amount of cracking, it can be defined as SCD. SCD is total length of cracks (μm) per unit area (μm^2) to evaluate the severity of cracking. Further, cracks can originate in either the HAZ or the recast layer. EDM process is very complex due to rapid local heating causing increase in local temperatures, more than melting point of material, results inimelting/vaporization followed by rapid cooling simultaneously followed by random attack of the spark. This results in the surface damage in the form of crack formation, along with generation of high thermal stresses exceeding the fracture strength of the material. The EDM surface undergoes chemical contamination, particularly carbon, from the electrode and dielectric fluid. From the metallurgical standpoint, carbon is considered as the most important contamination. Due to this, the brittleness of the white layer increases with increase in carbon contamination, which is favorable for crack formation. In spite of the presence of lot of cracks in the top surface, a few cracks penetrate through the transverse sections. These cracks, which are initiated at the top surface, propagate toward the parent material and diminish at the interface. This describes that the mechanism of crack formation is owing to solidification shrinkage during rapid cooling at the end of the spark discharge and not from the mechanical action of the spark [17]. The average of SCD-measured values from SEM photographs and their corresponding S/N ratio values are presented in the Table 7. The individual effect of process parameters such as peak current, surfactant concentration and graphite powder concentration on the mean values of SCD and S/N ratio for SCD are presented in Figs. 10 and 11. Further, it is observed from the Figs. 10 and 11 that SCD increases with increase in peak current. This may be due to the fact that increase in peak current increases spark energy, causing high amount of heat energy that penetrates into the work surface. This causes more localized temperatures, which induce higher thermal stresses due to rapid cooling. Further, it results in formation of more cracks, which penetrate deeper into the work surface, causing increase in SCD with increase in peak current. In addition to that it is also observed from Fig. 10 that there is significant increase in SCD with increase in surfactant concentration from 4 to 6 g/lt and then attains maximum value. Then decrease in SCD is noticed with further increase in surfactant concentration from 6 to 8 g/lt. The increase in concentration of surfactant in dielectric results in more concentrated spark energy and increase in localized temperatures at the work surface. Thus, SCD is increased. On the other hand, increase in surfactant

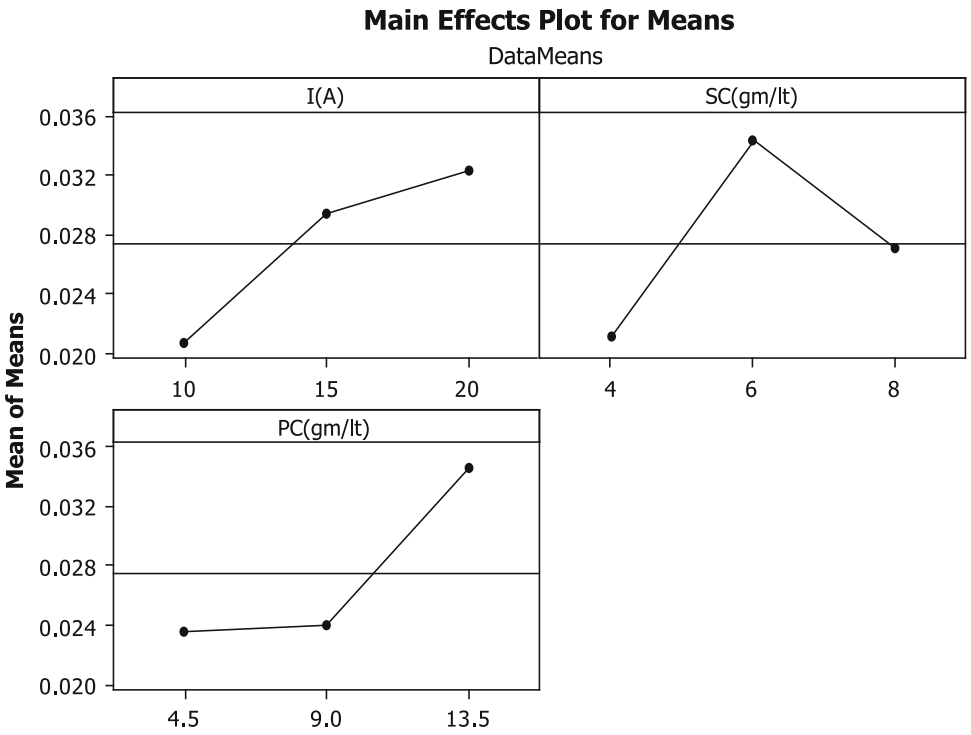

Fig. 10 The effect of process parameters on means of SCD

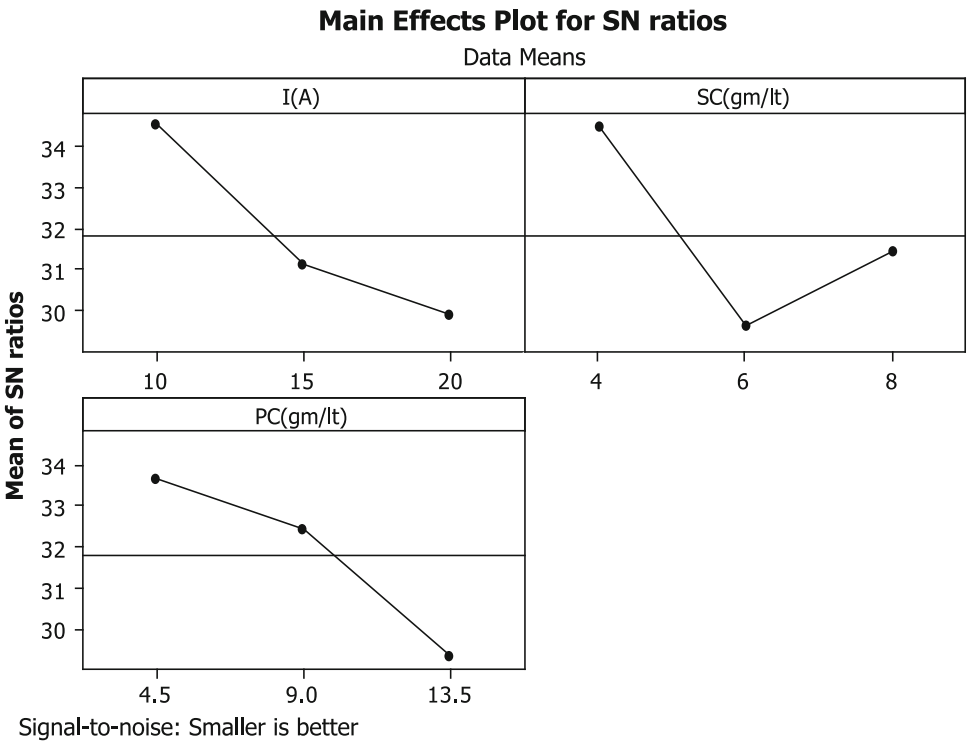

Fig. 11 The effect of process parameters on S/N Ratio of SCD

concentration may lead to increase in carbon enrichment into the molten pool during spark discharge, causing more brittle re-solidified layer. This results in increase in SCD. Further, it is noticed that there is decrease in SCD with increase in surfactant concentration from 6 to 8 g/lt. This may be due to dissipation of more amount of heat energy into the dielectric, which decreases SCD. However, surface cracks cannot be prevented by means of mechanical action of the particles because such cracks are formed due to high transformational strains developing during solidification

[7]. It is also noted from Fig. 10 that there is very small increase in SCD with increase in graphite powder concentration from 4 to 9 g/lt, whereas significant increase in SCD is found with increase in graphite powder concentration from 9 to 13.5 g/lt. This can be due to the deposition of more amount of carbon from graphite powder as well as from the dielectric into the molten puddle, which makes the white layer more brittle causing an increase in SCD.

Figure 11 suggests that SCD is observed to be minimum when the input parameters are peak current at 10 A (level 1), surfactant concentration at 4 g/lt (level 1) and graphite powder concentration at 4.5 g/lt (level 1). Further, the optimum SCD value is calculated as 0.10444 μm/μm^2, and corresponding S/N ratio value is 39.0252 at its optimal parameter setting.

It is observed from the Table 17 that all the three parameters are having significant effect on SCD. From the calculated F and P values, it is noticed that surfactant concentration is the most significant parameter followed by graphite powder concentration and peak current, which are more significant parameter, and significant parameter, respectively, affecting SCD.

Further, nonliner regression analysis is performed from the experimental data to predict response variable SCD. The regression coefficients of the model are presented in the Table 18. The R^2 (98.43 %) and R^2 adj (93.7 %) indicate satisfactory variability in the model in predicting the SCD. Further, the mathematical equation to predict SCD is

$$\begin{aligned}\text{SCD} = {} & -9.102556 + 0.004567I + 0.0325\text{SC} \\ & - 0.00337\text{PC} - 0.000113I^2 - 0.002583\text{SC}^2 \\ & + 0.000255\text{PC}^2 \end{aligned} \quad (5)$$

The predicted values of SCD using mathematical Eq. (5), and corresponding residuals are presented in the Table 19.

Table 17 Analysis of variance (ANOVA) for raw data SCD

Source	DF	Seq SS	Adj SS	Adj MS	*F*	*P*
I (A)	2	0.0002202	0.0002202	0.0001101	19.06	0.050
SC (g/lt)	2	0.0002676	0.0002676	0.0001338	23.15	0.041
PC (g/lt)	2	0.0002349	0.0002349	0.0001174	20.33	0.047
Error	2	0.0000116	0.0000116	0.0000058		
Total	8	0.0007342				

$S = 0.00240370$, $R^2 = 98.43$ % R^2 (adj) = 93.70 %

Table 18 Estimated Regression Coefficients for SCD

Term	Coef	SE Coef	*T*	*P*
Constant	−0.102556	0.021334	−4.807	0.041
I (A)	0.004567	0.002049	2.229	0.156
SC (g/lt)	0.032500	0.005123	6.344	0.024
PC (g/lt)	−0.003370	0.001526	−2.208	0.158
I^2	−0.000113	0.000068	−1.667	0.237
SC^2	−0.002583	0.000425	−6.080	0.026
PC^2	0.000255	0.000084	3.040	0.093

$S = 0.00240370$, PRESS = 0.000234, $R^2 = 98.43$ % R^2 (pred) = 68.13 % R^2 (adj) = 93.70 %

Table 19 Predicted values of SCD using regression model

EXP	*I* (A)	SC (g/lt)	PC (g/lt)	SCD (μm/μm^2)	FIT SCD	RESI
1	10	4	4.5	0.01	0.010	−0.000
2	10	6	9	0.023	0.024	−0.001
3	10	8	13.5	0.029	0.027	0.001
4	15	4	9	0.021	0.019	0.001
5	15	6	13.5	0.043	0.043	−0.000
6	15	8	4.5	0.024	0.025	−0.001
7	20	4	13.5	0.032	0.033	−0.001
8	20	6	4.5	0.037	0.035	0.001
9	20	8	9	0.028	0.028	−0.000

4 Confirmation experiments

To verify the predicted values of responses such as MRR, SR, WLT, and SCD at their optimal parametric settings, three confirmation experiments were conducted at their optimal parametric settings, and each experiment is repeated three times to take the average value. The data from the confirmation experiments and their comparisons with respective predicted values and the deviation of predicted

Table 20 Confirmation tests and their comparison with results

S No.	Optimum parameters			Response	Experimental value	Predicted value	% error
	I (A)	SC (g/lt)	PC (g/lt)				
1	20	6	9	Max.MRR (mm^3/min)	64.21	61.08	4.87
2	10	4	9	Min.SR (μm)	3.17	2.937	7.35
3	10	4	9	Min.WLT (μm)	14.1	13.445	4.64
4	10	4	4.5	Min.SCD (μm/μm^2)	0.01126	0.01045	7.19

results from experimental results are calculated as % error with Eq. (6) and are presented in Table 20.

$$\% \text{ error} = \frac{\text{experimental value} - \text{predicted value}}{\text{experimental value}} \times 100. \quad (6)$$

5 Conclusions

Based on the results obtained from experiments conducted in the present work, the following conclusions are drawn:

1. The addition of surfactant into the dielectric fluid increases dielectric conductivity, which shortens the relay time of discharge resulting in increase in MRR. The addition fine graphite particles into the dielectric may agglomerate due to electrostatic forces, leading to unstable machining. Surfactant molecules act as sterric barrier that separates agglomerated graphite powder particles and disperse them uniformly into the dielectric.
2. Peak current is most significant parameter affecting MRR, SR and WLT. However, it has significant effect on SCD. Surfactant concentration has significant effect on MRR, SR and WLT, whereas it has most significant effect on SCD. However, powder concentration has less significant effect on all response characteristics namely MRR, SR, WLT and SCD.
3. Further, in order to obtain optimum responses, the dominant process parameters are set: I at 10A, SC at 4 g/lt and PC at 9 g/lt yielding minimum SR (3.17 μm) and minimum WLT (14.1 μm), whereas I at 20A, SC at 6 g/lt and PC at 9 g/lt yielding maximum MRR (61.04 mm^3/min). However, when I is at 10 A, SC at 4 g/lt and PC at 4.5 g/lt, minimum SCD is obtained. Confirmation experiments were conducted at respective optimal parametric settings to verify predicted optimum values. The corresponding %error values are in the range of 4.64–7.35 %.

References

1. Beri N, Maheshwari S, Sharma C, Kumar A (2008) Performance evaluation of powder metallurgy electrode in electrical discharge machining of AISI D2 steel using Taguchi method. Int J Mech Ind Aerosp Eng
2. Kansal HK, Singh S, Kumar P (2005) Parametric optimization of powder mixed electrical discharge machining by response surface methodology. J Mater Process Technol 169:427–436
3. Guu YH, Hocheng H (2001) Effects of work piece rotation on machinability during electrical discharge machining. Mater Manuf Process 16:91–101
4. Chattopadhyay KD, Verma S, Satsangi PS, Sharma PC (2009) Development of empirical model for different process parameters during rotary electrical discharge machining of copper-steel (EN-8) system. J Mater Process Technol 209:1454–1465
5. Ghoreishi M, Atkinson J (2002) A comparative experimental study of machining characteristics in vibratory, rotary, and vibro: rotary electro discharge machining. J Mater Process Technol 120:374–384
6. Pecas P, Henriques E (2003) Influence of silicon powder mixed dielectric on conventional discharge machining. Int J Mach Tools Manuf 34:1465–1471
7. Bulent Ekmekci A, Tekkaya E, Erden A (2006) A semi-empirical approach for residual stresses in electric discharge machining (EDM). Int J Mach Tools Manuf 46:858–868
8. Kansal HK, Singh S, Kumar P (2006) Performance parameters optimization of powder mixed electrical discharges machining (PMEDM) by Taguchi method. West Indian J Eng 29:81–94
9. Khan AA (2008) Electrode wear and material removal rate during EDM of aluminum and mild steel using copper and brass electrodes. International Journal Advanced Manufacturing Technology 39:482–487
10. Payal HS, Choudhary R, Singh S (2008) Analysis of electro discharge machined surfaces of EN-31 tool steel. J Sci Ind Res 67:1072–1077
11. Choudhary R, Kumar H, Garg RK (2010) Analysis and evaluation of heat affected zones in electric discharge machining of EN-31 die steel. Indian J Eng Mater Sci 17:91–98
12. Shabgard M, Seyedzavvar M, Oliaei SNB (2011) Influence of input parameters on the characteristics of the EDM process. J Mech Eng 57:689–696
13. Jabbaripour B, Sadeghi MH, Shabgard MR, Faraji H (2013) Investigating surface roughness, material removal rate and corrosion resistance in PMEDM of γ- TiAl intermetallic. J Manuf Process 15:56–68
14. Bhattacharya A, Batish A, Kumar N (2013) Surface characterization and material migration during surface modification of die steels with silicon, graphite and tungsten powder in EDM process. J Mech Sci Technol 27:133–140
15. KL W, Yan BH, Huang FY, Chen SC (2005) Improvement of surface finish on SKD steel using electro discharge machining with aluminum and surfactant added dielectric. Int J Mach Tools Manuf 45:1195–1201
16. Dukhin AS, Goetz PJ, Ionic properties of so—called "non-ionic" surfactants in non-polar liquids, Dispersion Technology Inc., New York, pp 1–21.
17. Bhattacharyya B, Gangopadhyay S, Sarkar BR (2007) Modelling and analysis of EDMed job surface integrity. J Mater Process Technol 189:169–177